Friction of rodlike particles adsorbed to a planar surface in shear flow

Maria L. Ekiel-Jeżewska, Krzysztof Sadlej,[a] and Eligiusz Wajnryb
Institute of Fundamental Technological Research, Polish Academy of Sciences, ul. Świetokrzyska 21, 00-049 Warsaw, Poland

(Received 24 April 2008; accepted 20 June 2008; published online 25 July 2008)

A planar hard surface covered with elongated stiff rodlike particles in shear flow is considered in the low-Reynolds-number regime assuming low particle surface coverage. The particles are modeled as straight chains of spherical beads. Multipole expansion of the Stokes equations (the accurate HYDROMULTIPOLE algorithm) is applied to evaluate the hydrodynamic force exerted by the fluid on the rodlike particles, depending on their shape, i.e., on the number of beads and their orientation with respect to the wall and to the ambient shear flow. © *2008 American Institute of Physics*.
[DOI: 10.1063/1.2957492]

In recent years problems involving flows around microscale surface irregularities have become increasingly important in many applications. These include surface roughness effects in microchannels,[1] irreversible adsorption of particles and molecules on channel walls,[2–4] as well as biological and medical systems.[5,6] Depending on the problem encountered, it is of interest to determine the influence the shape of the surface irregularities has on quantities such as the total hydrodynamic resistance of a particle covered surface or the drag exerted on the individual particles. This provides a starting point for the study of moving, deformable polymers including Brownian motion, direct interparticle forces, and interactions with the boundaries.[7–9]

In this work we consider a system composed of rodlike particles of width $2a$ and length l, adsorbed on a solid, planar surface present at $z=0$. The particles are immersed in a shearing flow ($z>0$) of the form $\mathbf{v}_0=(z,0,0)$, where z and other coordinates are measured in units of a and the flow $\mathbf{v}_0$ is normalized by the fluid velocity u at a distance from the wall equal to a. The particle surface coverage is assumed to be small enough to treat them as noninteracting. Physically this means that the particles are spread apart by a distance several times larger than their dimensions. The influence of all adsorbed particles is then a sum of the effect of single particles.

The rodlike particle considered is modeled by a straight chain of $N=l/(2a)$ identical spherical solid beads of radius a (see Fig. 1), a method commonly used in literature.[10,11] The beads are in contact and do not move relative to each other forming a rigid rod.

Positions of the bead centers $\mathbf{R}_i$, $i=1, \ldots, N$, are parametrized by two angles $0\leq\phi\leq 2\pi$ and $0\leq\theta\leq\pi/2$, as shown in Fig. 1,

$$\mathbf{R}_i=\begin{pmatrix} 2(i-1)\sin\theta\cos\phi \\ 2(i-1)\sin\theta\sin\phi \\ 1+2(i-1)\cos\theta \end{pmatrix}. \tag{1}$$

The goal is to evaluate the force $\mathbf{F}(N,\theta,\phi)$, which is exerted by the fluid on the rodlike particle, depending on its orientation and aspect ratio $l/(2a)$. The force is measured in units of $6\pi\eta au$, where η is the viscosity of the fluid.

The derivation is based on the Stokes equations,[12]

$$\eta\nabla^2\mathbf{v}-\nabla p=\mathbf{0}, \quad \nabla\cdot\mathbf{v}=0, \tag{2}$$

for the fluid velocity $\mathbf{v}$ and pressure p. The stick boundary conditions hold at the solid-fluid interfaces, $\mathbf{v}=\mathbf{0}$, and the shearing ambient flow is assumed at an infinite distance from the particle, $\mathbf{v}=\mathbf{v}_0$.

Using the formalism of induced forces,[13–16] and Blake's expression[17] for the Green tensor in the considered system geometry, Eqs. (2) are transformed into a set of boundary integral equations at the surfaces of all the beads.[12] These equations are next projected onto a complete set of spherical multipole functions.[18–21] The resulting infinite system of algebraic equations is truncated at a multipole order L,[22] which corresponds to taking $3L(L+2)$ multipoles per bead. For the precise definition of L, see Ref. 23. The force multipoles of each bead are then evaluated. In particular, the lowest multipoles correspond to the forces exerted by the fluid on the beads $i=1, \ldots, N$; their sum results in the total force $\mathbf{F}$ exerted on the rodlike particle,

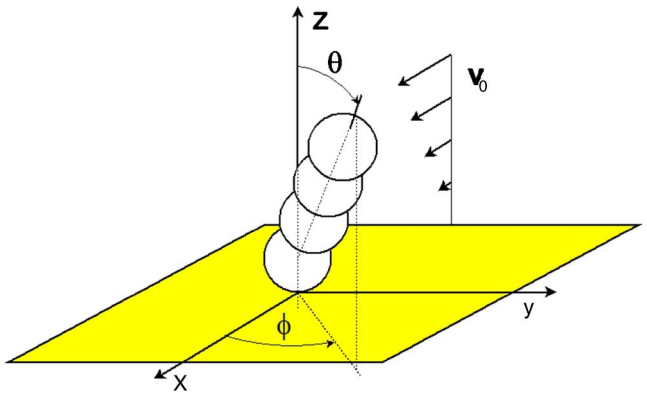

FIG. 1. (Color online) Rodlike particle attached to a planar solid wall in shear flow.

[a]Electronic mail: ksadlej@ippt.gov.pl.

$$\mathbf{F} = \sum_{i=1}^{N}\sum_{j=1}^{N} \begin{pmatrix} \zeta_{ij}^{tt} & \zeta_{ij}^{tr} & \zeta_{ij}^{td} \end{pmatrix} \cdot \begin{pmatrix} \mathbf{v}_{0j} \\ \boldsymbol{\omega}_{0j} \\ \mathbf{g}_{0j} \end{pmatrix}, \tag{3}$$

where $\mathbf{v}_{0j}=\mathbf{v}_0(\mathbf{R}_j)$, $\omega_{0j}=\frac{1}{2}\nabla\times\mathbf{v}_0(\mathbf{r})|_{\mathbf{r}=\mathbf{R}_j}$, and $\mathbf{g}_{0j,\alpha\beta}=\frac{1}{2}[\nabla_\alpha \mathrm{v}_{0\beta}(\mathbf{r})+\nabla_\beta \mathrm{v}_{0\alpha}(\mathbf{r})]_{\mathbf{r}=\mathbf{R}_j}$.

The friction matrices $\boldsymbol{\zeta}_{ij}^{tp}$, with $p=t,r,d$, depend on the particle orientation with respect to the wall and are evaluated by the well-known procedure, described in Refs. 18 and 24 and implemented in the HYDROMULTIPOLE numerical code.[23] For a motionless system of particles, lubrication phenomena are absent, and the convergence of the multipole expansion with the order of the truncation L is typically fast.[22,25]

The derivation of the friction force $\mathbf{F}$ significantly simplifies owing to linearity of the Stokes equations. The point is to decompose the ambient flow $\mathbf{v}_0$ into two components, perpendicular and parallel to the plane which contains the centers of all the beads and the normal to the wall. Then, $\mathbf{F}$ is constructed as the superposition of the forces caused by these two components of $\mathbf{v}_0$. In addition, the symmetry of the system and of the Stokes equations under geometrical reflections and time-reversal (i.e., $\mathbf{v}\to-\mathbf{v}$ and $p\to-p$) is taken into account. Finally, the hydrodynamic force $\mathbf{F}$ is expressed in terms of three scalar functions $\alpha(\theta,N)$, $\beta(\theta,N)$, and $\gamma(\theta,N)$, with the explicit dependence on $0\le\phi\le2\pi$,

$$\boldsymbol{F}(N,\theta,\phi) = \begin{pmatrix} \alpha(\theta,N)\sin^2\phi + \beta(\theta,N)\cos^2\phi \\ [\beta(\theta,N)-\alpha(\theta,N)]\sin\phi\cos\phi \\ \gamma(\theta,N)\cos\phi \end{pmatrix}. \tag{4}$$

The functions $\beta(\theta,N)$ and $\gamma(\theta,N)$ are the only nonzero force components (along the ambient flow and normal to the wall, respectively), if $\phi=0$. On the other hand, $\alpha(\theta,N)$ is the only nonzero force component (along the ambient flow), if $\phi=\pi/2$.

The functions $\alpha(\theta,N)$, $\beta(\theta,N)$, and $\gamma(\theta,N)$ have been evaluated numerically using the HYDROMULTIPOLE algorithm.[18] The mentioned parameter of truncation L has been chosen equal to 5. This is sufficient to obtain a precision better than 0.1%, estimated by comparing the values of α, β, and γ, calculated for multipole truncation orders L equal to $5,6,\ldots,20$ and retaining only the digits which remain constant when changing L.

Obviously, the hydrodynamic force increases when the number of beads is increased. Therefore it is of interest to evaluate the fore per bead $\mathbf{F}/N$. It corresponds to the fore per "segment" of the rodlike particle. The corresponding coefficients α/N, β/N, and γ/N are plotted in Fig. 2 as functions of θ, for a given number of beads ($N=1,2,4,6,8,10$).

The force components along the ambient flow, α (for $\phi=\pi/2$) and β (for $\phi=0$), decrease with the increase in θ. A rodlike particle sticking out of the wall undergoes a higher ambient flow (and therefore a higher hydrodynamic force per segment) than a particle in a flat contact with the wall. In Figs. 2(a) and 2(b), the discussed functions $\alpha(\theta,N)/N$ and $\beta(\theta,N)/N$ are compared to the force exerted on a single spherical particle, $\alpha(\theta,1)=\beta(\theta,1)\equiv1.7009$.[26] Note that at values of θ close to zero when the particle axis is normal to the wall, the force along the flow exerted per segment of the particle is significantly larger than for a single sphere, as on average each segment is immersed in a flow of higher velocity. On the other hand, for θ close to $\pi/2$, due to screening, these functions take values always smaller than the force exerted on a single spherical particle.

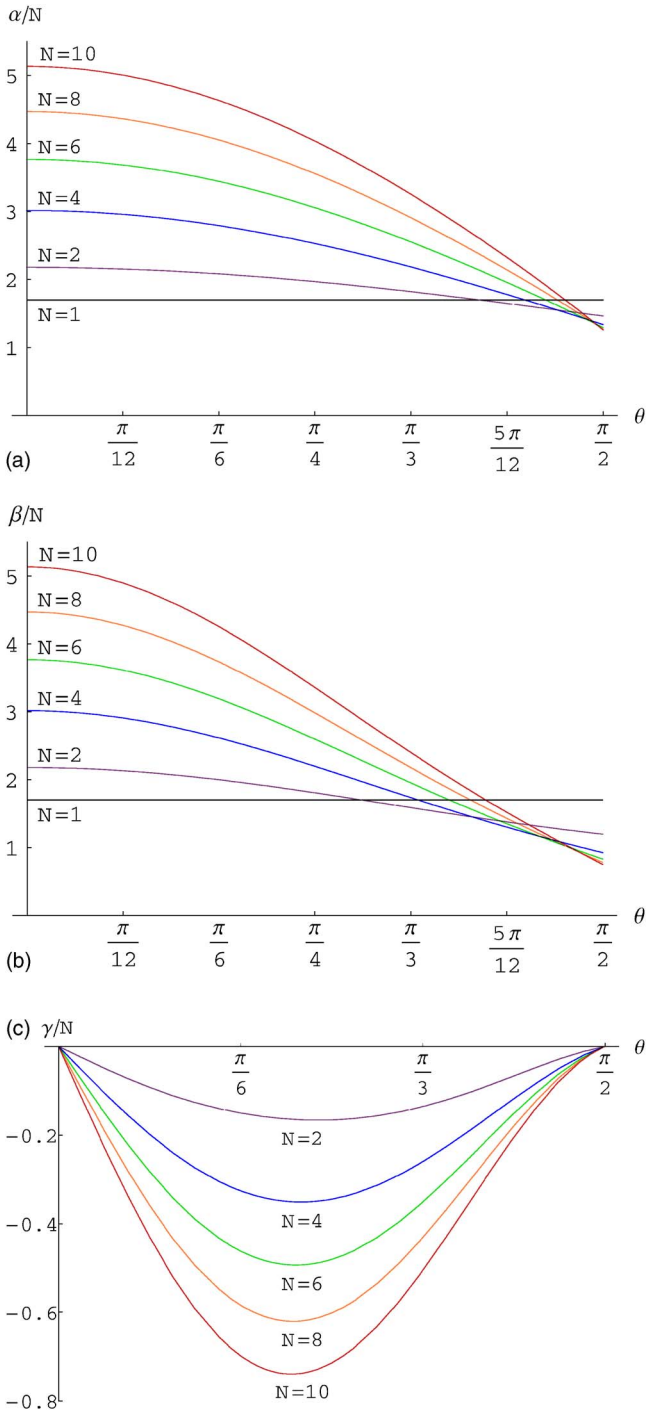

FIG. 2. (Color online) Force exerted by the fluid per segment of the rodlike particle in shear flow, F/N. Top: the component along the flow for $\phi=\pi/2$. Middle: the component along the flow for $\phi=0$. Bottom: the component normal to the wall for $\phi=0$.

On the other hand, the force component normal to the wall, γ [see Fig. 2(c)], vanishes if the particle's orientation is perpendicular or parallel to the wall. This component is also equal zero for $N=1$. The maximum of $|\gamma|$ for $N>1$ is

TABLE I. The friction force exerted by the fluid on a segment of an adsorbed particle. Parts 1 and 2: At different orientations; part 3: Averaged over a uniform distribution of configurations [$\bar{F}(N)$: Averaged over θ and ϕ; $\bar{F}_{\mathrm{Q2D}}(N)$: Averaged over ϕ for particles adsorbed flat on the wall].

N	1	2	4	10	20	40	100
$\theta_{\max}$	⋯	0.72	0.70	0.67	0.66	0.65	0.64
$\gamma(\theta_{\max},N)/N$	0	−0.17	−0.35	−0.74	−1.27	−2.21	−4.68
$\beta(\theta_{\max},N)/N$	1.70	1.86	2.35	3.77	5.86	9.56	19.17
$\alpha(\pi/2,N)/N$	1.70	1.46	1.34	1.26	1.23	1.22	1.21
$\beta(\pi/2,N)/N$	1.70	1.20	0.93	0.75	0.69	0.66	0.64
$\alpha(0,N)/N$	1.70	2.18	3.02	5.14	12.24	20.21	40.97
$\bar{F}(N)/N$	1.70	1.72	2.00	2.91	4.29	6.76	13.19
$\bar{F}_{\mathrm{Q2D}}(N)/N$	1.70	1.33	1.14	1.01	0.96	0.94	0.93

reached at $\theta_{\max}$. The values of $\theta_{\max}$ for particles with different aspect ratios N can be found in the first part of Table I, together with the hydrodynamic force for the orientation $\theta=\theta_{\max}$ and $\phi=0$. Notice that $\theta_{\max}$ is a decreasing function of N and that $|\gamma/\beta|$ at $\theta_{\max}$ is an increasing function of N. The negative sign of γ means that for $\phi<\pi/2$ the force normal to the wall is directed toward it, pushing the particle onto the wall.

The component along the flow gives the dominant contribution to the total force (for $\phi=0$, compare the plots of β and γ in Fig. 2 and notice their different scales). Nevertheless the larger the values of N, the more significant is the contribution to the total force coming from the direction normal to the wall.

The following three characteristic orientations of the rodlike particle are analyzed in greater detail for a wider range of N: (a) $\phi=0$, $\theta=0$ (perpendicular to the wall), (b) $\phi=0$, $\theta=\pi/2$ (parallel to the wall and parallel to the ambient flow), and (c) $\phi=\pi/2$, $\theta=\pi/2$ (parallel to the wall and perpendicular to the ambient flow). For each of these orientations, the force per bead F/N, equal, respectively, to $\alpha(0,N)/N$, $\beta(\pi/2,N)/N$, and $\alpha(\pi/2,N)/N$, has been evaluated. The results are listed in the second part of Table I and plotted in Fig. 3.

For the particle perpendicular to the wall, the force per bead increases with large N, while for the particle adsorbed flat at the wall, it saturates at a constant value. A more careful investigation of the asymptotic behavior of these quantities results in the following scalings:

$$\alpha(0,N)/N \approx \frac{4N}{3(\log N + 0.30)}, \tag{5}$$

$$\alpha(\pi/2,N)/N \approx 1.21 \pm 0.01 + \mathcal{O}(1/N), \tag{6}$$

$$\beta(\pi/2,N)/N \approx 0.63 \pm 0.03 + \mathcal{O}(1/N). \tag{7}$$

The first formula (5), for the rodlike particle perpendicular to the wall, has been derived from calculations with a multipole order $L=5$ and N equal up to 1800. It is consistent in form with the result $4N/[3(\log N+A)]$ for infinite space,[13,27] as for large distances from the wall the effects of the shearing flow dominate the influence of the wall. The constant A depends nevertheless on the geometry of the system. For the bead model in infinite space $A=0.97$,[22] while in the presence of the wall $A=0.30$.

The remaining two formulas (6) and (7) for particles adsorbed flat on the surface have been calculated for multipole orders $1\leqslant L\leqslant 5$ and number of beads $1300\geqslant L\geqslant 110$, respectively. In this case the influence of the wall is dominant.

In real systems the orientation of particles is often random. The exerted force which is then of interest is a value averaged over all possible orientations with a uniform distribution function for all $0\leq\phi<2\pi$ and $0\leq\theta\leq\pi/2$. It is given by the formula

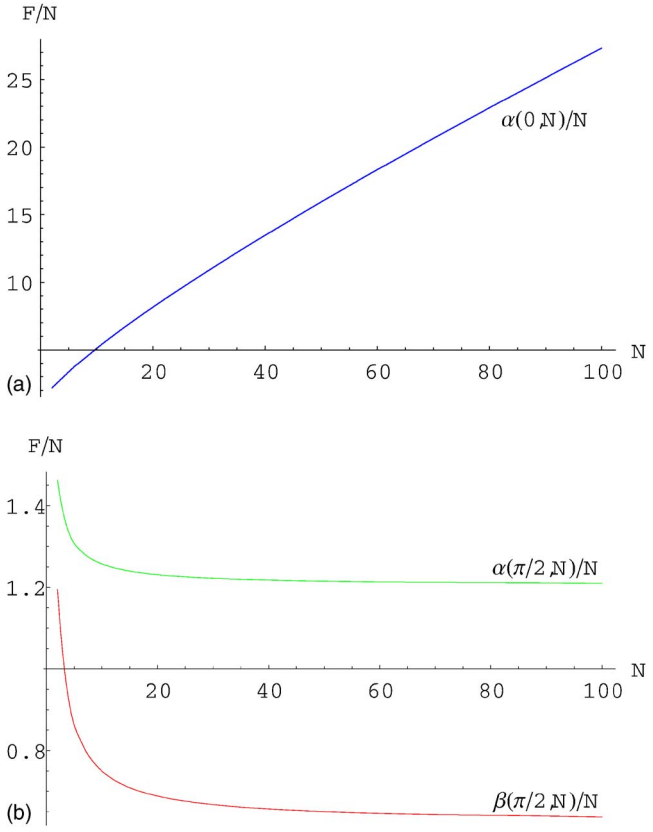

FIG. 3. (Color online) Friction force exerted by the fluid per segment of the adsorbed particle.

$$\bar{\boldsymbol{F}}(N) = \int_0^{\pi/2} d\theta \sin\theta \left(\frac{1}{2\pi} \int_0^{2\pi} d\phi \boldsymbol{F}(N,\theta,\phi) \right), \tag{8}$$

where $\boldsymbol{F}(N,\theta,\phi)$ is provided by Eq. (4). Note that only the component of the averaged force parallel to the ambient flow direction is different from zero. This can be deduced from symmetries of the system or derived directly from Eq. (4) by analytically calculating the integrals over ϕ of the trigonometric functions. In general, the calculation of the integral (8) is split into two stages. First, the averaging over the angle ϕ is performed resulting in the function $(\alpha(\theta,N)+\beta(\theta,N))/2$. Its values for different angles θ and number of segments N are evaluated using the HYDROMULTIPOLE algorithm[18] as already discussed. Multipole truncation order is chosen to $L=5$ resulting in the accuracy of the integrand function better than 0.1%. Integration over θ is then performed using the Gauss method implemented within the NUMERICAL RECIPES package. The number of Gauss points is chosen equal to 10, which is enough to obtain a precision of 10^{-5} of the integration procedure. The values of the averaged force $\bar{F}(N)$ obtained for different aspect ratios of the rodlike particle have been listed in the third part of Table I.

In practical applications, apart from totally random particle orientations, one encounters also systems in which particles are adsorbed flat on the surface, retaining only the randomness in the angle ϕ between their axis and the flow direction. This system is quasi-two-dimensional. The average force exerted on the particle is then given by the expression in brackets in Eq. (8) taken at $\theta=\pi/2$. It is parallel to the flow direction and given by

$$\bar{F}_{\mathrm{Q2D}}(N) = \frac{1}{2}\left[\alpha\left(\frac{\pi}{2},N\right) + \beta\left(\frac{\pi}{2},N\right) \right]. \tag{9}$$

The values of $\bar{F}_{\mathrm{Q2D}}(N)$ obtained for different aspect ratios of the particle have been listed in the third part of Table I.

Concluding, in this work we have calculated the friction force exerted by the shear flow on an adsorbed rodlike polymer, depending on its orientation with respect to the flow direction. The multipole method used offers a well defined mechanism of controlled precision[25] through the change of the multipole cutoff number L. It enabled us to determine very precisely the hydrodynamic effects of the wall on elongated particles. These results may also be used to test simpler models and applied in may contexts.[9,28–30] Finally, we have found that the averaged force $\bar{F}_{\mathrm{Q2D}}(N)$ of a rodlike particle composed of N spherical particles adsorbed flat on the surface is significantly smaller then the total friction force of N isolated adsorbed spherical particles. This means that once particles group into elongated structures, the flow exerts a much smaller force on them. This observation might have broader implications for the understanding of the dynamics of self-assembling quasi-two-dimensional systems.

We thank Z. Adamczyk and P. Warszyński for discussions. This work was partially supported by the MANAR Network financed by the Polish Ministry of Science and Higher Education.

[1] G. Gamrat, M. Favre-Marinet, S. Le Person, R. Baviere, and F. Ayela, J. Fluid Mech. **594**, 399 (2008).
[2] R. G. Larson, T. T. Perkins, D. E. Smith, and S. Chu, Phys. Rev. E **55**, 1794 (1997).
[3] D. J. Olson, J. M. Johnson, P. D. Patel, E. S. G. Shaqfeh, S. G. Boxer, and G. G. Fuller, Langmuir **17**, 7396 (2001).
[4] T. T. Perkins, D. E. Smith, and S. Chu, Science **276**, 2016 (1997).
[5] Z. Adamczyk, *Particles at Interfaces: Interactions, Deposition, Structure* (Academic, New York, 2006), Vol. 9.
[6] R. J. Hunter, *Foundations of Colloid Science* (Oxford University Press, New York, 2001).
[7] A. Alexander-Katz and R. R. Netz, Europhys. Lett. **80**, 18001 (2007).
[8] R. Delgado-Buscalioni, Phys. Rev. Lett. **96**, 088303 (2006).
[9] C. M. Schroeder, E. S. G. Shaqfeh, and S. Chu, Macromolecules **37**, 9242 (2004).
[10] J. K. G. Dhont and W. J. Briels, *Rod-Like Brownian Particles in Shear Flow* (Wiley, Berlin, 1988).
[11] M. Doi and S. F. Edwards, *The Theory of Polymer Dynamics*, reprint ed. (Clarendon, Oxford, 1988).
[12] S. Kim and S. J. Karilla, *Microhydrodynamics: Principles and Selected Applications* (Dover, Mineola, NY, 2005).
[13] R. G. Cox and H. Brenner, J. Fluid Mech. **28**, 391 (1967).
[14] B. U. Felderhof, Physica A **84**, 557 (1976).
[15] B. U. Felderhof, Physica A **84**, 569 (1976).
[16] P. Mazur and D. Bedeaux, Physica (Amsterdam) **76**, 235 (1974).
[17] J. R. Blake, Proc. Cambridge Philos. Soc. **70**, 303 (1971).
[18] B. Cichocki, R. B. Jones, R. Kutteh, and E. Wajnryb, J. Chem. Phys. **112**, 2548 (2000).
[19] B. U. Felderhof and R. B. Jones, Physica A **93**, 457 (1978).
[20] R. Schmitz and B. U. Felderhof, Physica A **92**, 423 (1978).
[21] R. Schmitz and B. U. Felderhof, Physica A **113**, 90 (1982).
[22] B. Cichocki, B. U. Felderhof, K. Hinsen, E. Wajnryb, and J. Blawzdziewicz, J. Chem. Phys. **100**, 3780 (1994).
[23] B. Cichocki, M. L. Ekiel-Jeżewska, and E. Wajnryb, J. Chem. Phys. **111**, 3265 (1999).
[24] B. Cichocki and R. B. Jones, Physica A **258**, 273 (1998).
[25] M. L. Ekiel-Jeżewska and E. Wajnryb, Q. J. Mech. Appl. Math. **59**, 563 (2006).
[26] M. E. O'Neill, Chem. Eng. Sci. **23**, 1293 (1968).
[27] J. Happel and H. Brenner, *Low Reynolds Number Hydrodynamics* (Martunus Nihhoff, Dordrecht, 1986).
[28] N. Hoda and S. Kumar, J. Chem. Phys. **127**, 234902 (2007).
[29] R. M. Jendrejack, E. T. Dimalanta, D. C. Schwartz, M. D. Graham, and J. J. de Pablo, Phys. Rev. Lett. **91**, 038102 (2003).
[30] C. Sendner and R. R. Netz, Europhys. Lett. **81**, 54006 (2008).